On the Aerodynamics of Bicycle Wheels*

Alexander I J Forrester†
Computational Engineering and Design Group
School of Engineering Sciences
University of Southampton SO17 1BJ
UK

January 2, 2008

Keywords: cycling, drag, disc wheel, tri-spoke, spokes

Abstract

Cyclists routinely vary the configuration of the wheels on their bicycles in order to change the weight, stiffness, strength and drag. However, while weight, stiffness and durability can be easily assessed, wheel selection for low drag tends to be based on gut feeling and, more often than not, wheel manufacturers' publicity. Here, a set of generic bicycle wheels have been tested in a wind tunnel in order to assess which general configurations work best and to quantify the differences in drag between various wheels. Results indicate that there can in fact be a reduction in power required to drive the wheel for an increase in number of spokes. It is also found that the more fashionable disc and tri-spoke wheels do not perform as well as traditional wire spoked wheels. A comparison of the power required to drive the wheels and the total power to propel the bicycle and rider shows that changes in wheel configuration can be as important as variations in rider position.

*This paper is based on results from experiments conducted in 2000 for the author's third year undergraduate project.

†Lecturer, School of Engineering Sciences

Nomenclature

C_D	drag coefficient of wheel
C_{DL}	longitudinal component of C_D
C_{DR}	rotational component of C_D
D	drag of wheel (N)
D_L	longitudinal component of D (N)
D_R	rotational component of D (N)
P	power to overcome drag of wheel (W)
P_L	power to overcome longitudinal component of D (W)
P_R	power to overcome rotational component of D (W)
S	area of wheel (m^2)
ω	angular velocity of wheel ($rad \cdot s^{-1}$)
ρ	density of air ($kg \cdot m^{-3}$)
r	radius of wheel (m)
U_B	velocity of bicycle ($km \cdot hr^{-1}$)
U_W	velocity of wind (relative to a stationary observer) ($km \cdot hr^{-1}$)
U_∞	freestream velocity (relative to rider) ($U_B + U_W$) ($km \cdot hr^{-1}$)
$\emptyset$	spoke diameter (m)

1 Introduction

The importance of aerodynamics first hit professional cycling when Greg Lemond won the 1989 Tour de France from Laurent Fignon by taking the last stage on the Champs Elyses with a new handlebar setup and streamlined helmet. Since then, the Scottish underdog Graham Obree broke the cycling status quo with his novel aerodynamic riding positions, breaking the hour record twice and winning two world titles. After Chris Boardman smashed the world hour record using Obree's 'Superman position', cycling's governing body (the UCI) brought in rules to restrict the positions riders can use. There are also rules regulating the use of aerodynamic monocoque frames, such as the Lotus frame used by Chris Boardman in the 1992 Barcelona Olympics. There is now a new 'best human

effort' record where riders must use more primitive equipment, similar to that used by Eddy Merckx in 1972.

So far, however, there have been no severe limitations on the type of wheel that is used (outside of the hour record). Competitors are free to choose rim profile, spoke numbers and profiles, and even use a solid wheel in many races. The restrictions on wheel configuration is dependent on the type of race, with three categories: 1) hour record, with 16 to 32 spokes and a rim with width and depth no greater than 22 mm; 2) massed start races, with greater than 12 spokes; and 3) individual and track races, no restrictions (UCI, 2005).

There is an obvious tradeoff between using fewer spokes for weight saving and more for durability, and this is likely to be decided by the type of rider and the course. However, the relationship between wheel configuration and aerodynamic drag is less obvious. While there have been startling displays of how position and helmet (or head fairing) shape can turn the tide in races, there is little evidence as to which wheel configuration is optimal and how much impact the wheel has on the performance of the rider. This paper presents an experimental investigation into the effect of various wheel configurations. Data is available on the performance of various commercially available wheels (Greenwell et al., 1995; Tew and Sayers, 1999), but here a generic wheel is used throughout in order that configuration changes can be quantified – e.g. the number of spokes can be changed while using the same rim and hub.

The next section shows how the drag of the wheel is measured through the experimental setup. Section 3 looks at the results obtained and what these mean when compared with the overall drag of the bicycle and rider. Conclusions are then drawn in the final section.

2 Experimental setup

The force required to move a wheel forwards is split into two components which we can measure in the wind tunnel. The first component is the reaction required to hold the axle of the spinning wheel stationary in the tunnel against the force of the oncoming wind, D_L, as shown in figure 1. This this is easily measured using the wind tunnel balance (as F_{balance}) and is sometimes the only force considered in wind tunnel tests (e.g. (Sayers

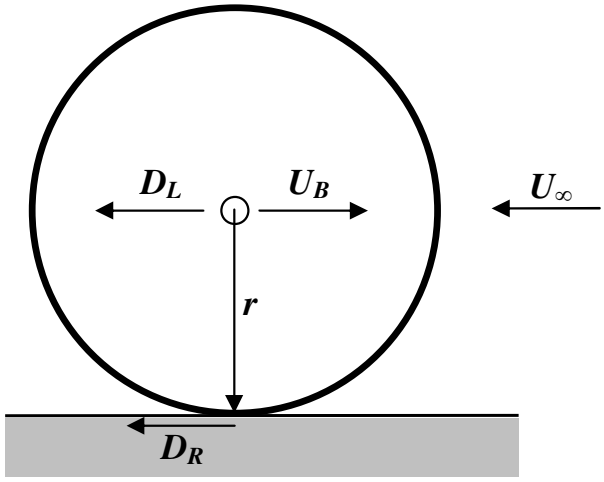

Figure 1: Components of drag on the bicycle wheel.

and Stanley, 1994; Greenwell et al., 1995; Tew and Sayers, 1999)). Additionally, there is also a force required to *rotate* the wheel acting against the circumferential component of the drag. This drag is overcome by the road pushing backwards on the wheel with the torque $D_R r$, with an equal and opposite forward force at the hub. Since there is no ground in our wind tunnel test, this is measured using the power, P_{motor}, required to turn the wheel using an electric motor. Thus the total aerodynamic drag of the wheel, $D = D_L + D_R = F_{\text{balance}} + P_{\text{motor}}/U_B$.

Experiments were carried out in a 0.61m $\times$ 0.61m tunnel using half scale wheels with the tunnel speed and wheel rotation doubled to give Reynolds number equivalence to full scale wheels. In the remainder of the paper we will refer to full scale velocities, forces and powers. A solid aluminium ring represents the rim and tyre and is attached to a hub via six wire spokes with adjustable tension to allow the rim and hub centres to be aligned ('trued'). The large momentum of this heavy rim facilitates operation at constant velocities. Further spokes are bonded to the rim and hub with cyanoacrylate adhesive. This setup allows one spoke to be added in each of the gaps between the existing spokes to give $N_S = 12$ and 24, or two spokes to be added in each gap to give $N_S = 18$ followed by one spoke in each gap for $N_S = 36$. It should be noted here that only cylindrical spokes have been tested. Oval or aerofoil spokes may provide improved drag characteristics when carefully aligned

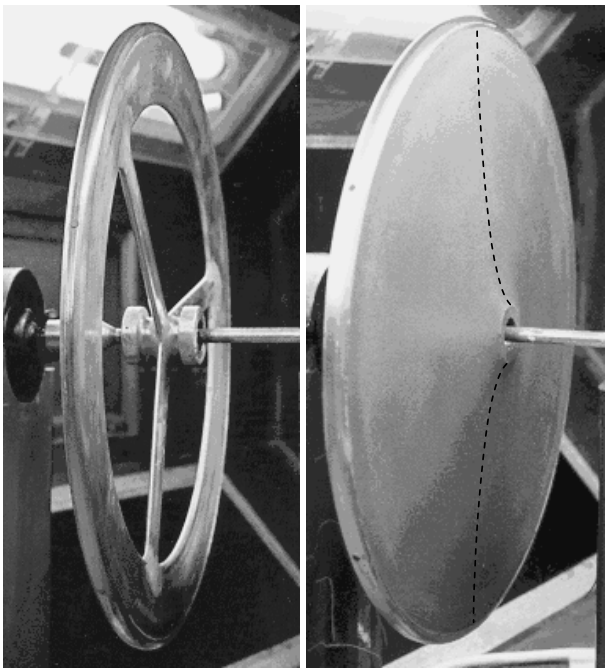

Figure 2: Test wheel in tri-spoke and disc configuration. Dashed lines show the concave shape of the disc sides.

to the flow to avoid stall. However, here general configurations are considered rather than detailed examination of individual setups.

Experiments have also been conducted using 'tri-spoke' and disc wheel configurations. The tri-spoke was built using three extruded aluminum tubes with a thick aerofoil cross section. These were bonded to the rim with epoxy resin and filleted with polyester filler – as seen in figure 2. The six wire 'truing' spokes were then removed and the holes plugged. The sides of the disc wheel were fabricated using tissue paper stiffened with cellulose dope (with the six truing spokes remaining inside the wheel). This construction results in the concave sides seen in figure 2.

The wheel is rotated via a 30 V DC motor, controlled with a variac, with an ammeter in series and a voltmeter in parallel to allow power measurement. A commercial cycle computer is used to measure U_B. The test rig is mounted on a mechanical balance located beneath the tunnel. Forces are measured via a sliding mass system to an accuracy of ± 0.1

N. Tare values are taken to account for the drag of the test rig and the efficiency of the motor. The effect of the flow being constrained within the tunnel (blockage) is corrected for using empirical rules from Freeman (1980). The tunnel used has no revolving road and so the effect of the ground cannot be taken into account. It is unlikely that the ground would have a large effect on the aerodynamic drag since the wheel is stationary where it meets the ground, with the majority of the drag coming form the fast, upper portion of the wheel.

3 Results

Tests were performed with the spoked wheel for $N_s = 6, 12, 18, 24$ and the disc and tri-spoke wheels at $U_B = 10, 20, 30, 40, 60$ and $U_W = 0, 10, 20, 30, 40$ (U_W being limited by the power of the wind tunnel).

Figure 3 shows P_L for varying U_B and U_W for each wheel configuration. The data is fitted using a statistical modelling method known as *kriging* (see, e.g. (Jones, 2001)), which allows us to filter experimental error, but still accommodate unusual responses by maximising the likelihood of the data. Using this method we can extract trends from the data, rather than prescribing them, e.g. by fitting a polynomial model.

For the wire spoked wheels the power rises from 6 to 12 to 18 spokes, as would be expected. However, for the 24 spoke wheel the power drops back to levels similar to those for 18 spokes. The number of spokes has a significant impact on the form of the power / velocity surfaces in figure 3. We would normally expect to see an increase in power proportional to the velocity cubed, and this trend is indeed seen in the disc and 18 spoke plots. The tri-spoke, 6, 12 and 24 spoke plots display a more linear trend. The flow over a spinning wheel is naturally more complex than that over a solid body (where $D \propto U^2$) and it is likely that varying interaction between turbulence shed by the spinning spokes and the flow over the wheel is the reason for the differing trends.

Disc wheels and tri-spokes are a popular choice amongst athletes, appearing to offer a much more streamlined profile to the wind, but the data in figure 3 does not indicate any advantage over wire spoked wheels in terms of the P_L component.

The P_L results must be coupled with the effort required to turn the wheel, which is measured as P_R, as displayed in figure 4. More consistent trends are seen in the P_R data, although this is likely to be partly due to the increased accuracy of measurement using a digital voltmeter and ammeter – note how close the data lies to the surface in comparison to the P_L data in figure 3. We *do*, however, still see the same pattern in terms of wheel configuration. The power increases with spoke number from six through to 18 spokes and then drops for 24. The disc and tri-spoke wheels are comparatively better, with similar P_R levels to the six spoke wheel. Another difference between the P_R and P_L trends is that P_R is more strongly related to U_B than U_W, with P_L being affected more by U_W. This follows intuition, since P_L is in the direction of U_W and P_R is a torque multiplied by the angular velocity, $\omega = U_B r$.

We now put the two components together to give $P = P_L + P_R$, the result of which is shown in figure 5. These plots of the total power required to move the wheel at U_B into U_W accentuate the difference between the wheel configurations. D_L is the overriding component contributing to P, but the inclusion of P_R introduces a stronger relation between P and U_B than would be present by simply measuring D_L.

It is worth noting at this point that the poor performance of the disc and tri-spoke wheels does not necessarily indicate that these configurations are inferior. One form of disc wheel with concave sides and one profile of aerofoil spokes have been tested. Different profiles will produce different results which may, of course, improve on our results. It is perhaps more interesting though to concentrate on the issue of spoke number, since this can be varied and visualised more easily than disc shape or aerofoil profile.

To examine the behaviour of N_s more closely, P for varying U_B and N_s at $U_W = 0$ is plotted in figure 6. Further experiments have been conducted with $N_S = 36$ to confirm that there is, as expected, a rise in P beyond the drop for $N_S = 24$. It is clear from figure 6 that the number of spokes is largely immaterial below 20km/hr, e.g. for uphill races, but above this point N_S significantly affects P. Also note that each set of data for a given N_S exhibits the type of trend we would expect of $P \propto U_B^3$. We can in fact extract a drag coefficient for a given number of spokes by fitting a cubic to each set of data.

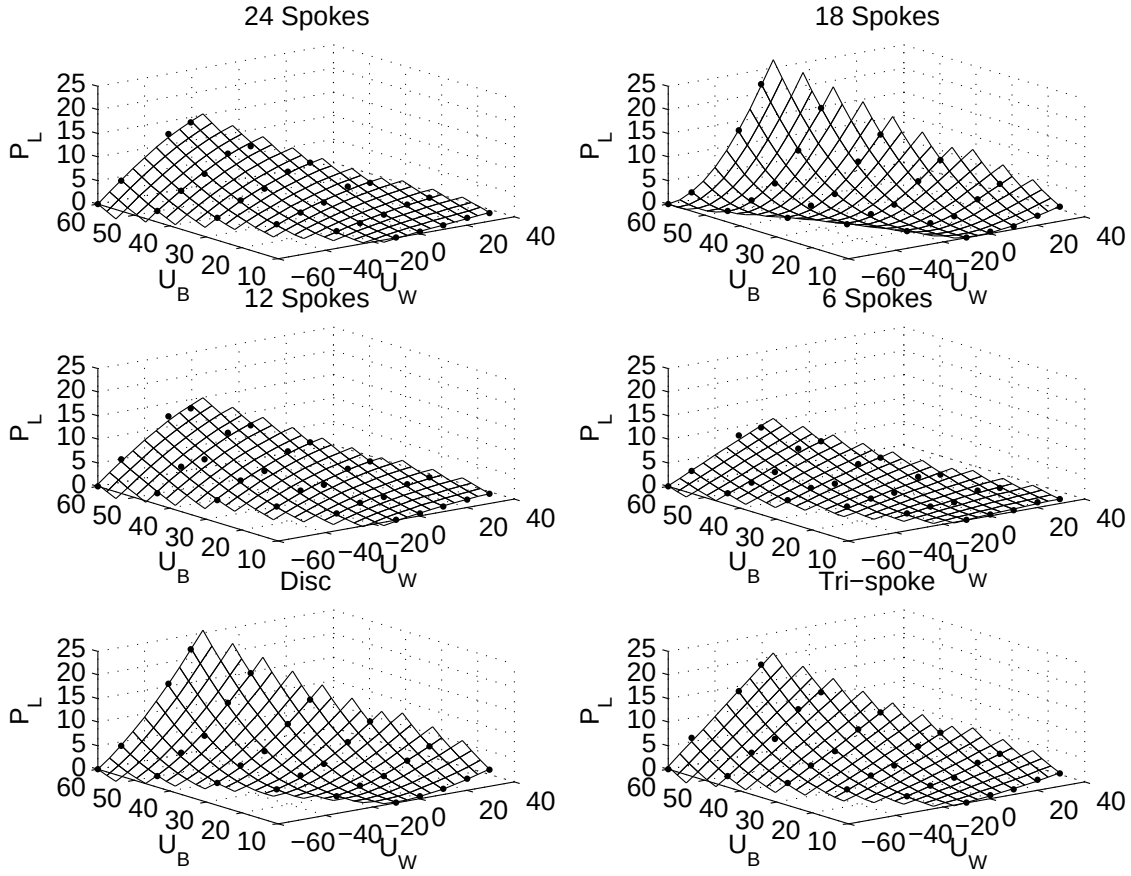

Figure 3: P_L for each configuration at varying U_B and U_W.

Defining a coefficient of drag for the wheel as:

$$C_D = \frac{2P}{\rho U_\infty^3 S}, \tag{1}$$

C_D is found from a least squares fitting of the drag data for each number of spokes, i.e.

$$C_D = \frac{2(\mathbf{U}^T\mathbf{U})^{-1}\mathbf{U}^T\mathbf{P}}{\rho S}, \tag{2}$$

where $\mathbf{U}$ is a vector of the test velocities cubed and $\mathbf{P}$ is a vector of the corresponding powers. Now the effect of the number of spokes can be seen more clearly in figure 6 where C_D is plotted against N_s. Error bars indicate the error in the least squares fitting and the drag measurement error.

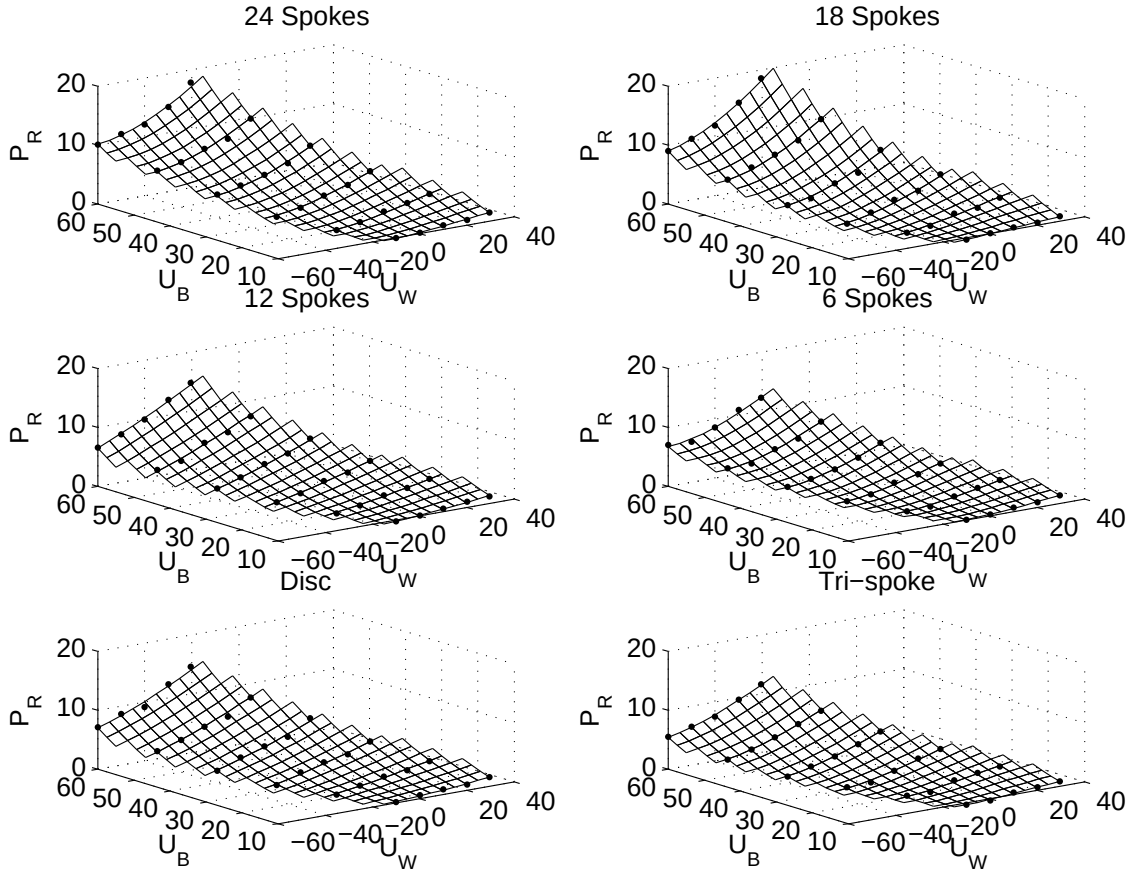

Figure 4: P_R for each configuration at varying U_B and U_W.

It is clear that for this wheel there is an optimum number of spokes somewhere between 18 and 36. Only $N_s = 24$ has been tested in this range, and $N_s = 28$ is the only other number of spokes for which hubs and rims are available, due to commonly used spoke 'lacing' patterns. However, a radially spoked wheel (for front wheel use only, due to torque transmitted from the hub in the rear wheel) with any even number of spokes may be produced and such a wheel may of course perform better than our 24 spoke example. However, testing 20, 22, 26, 28 and 32 spoke wheels would require individually machined hubs and rims for the different numbers of truing spokes required. The apparent 'critical spoke number' where this drag reduction paradox is seen for our wheel may not occur on all wheels, and if it does, will not necessarily be at the same N_s. The explanation for the

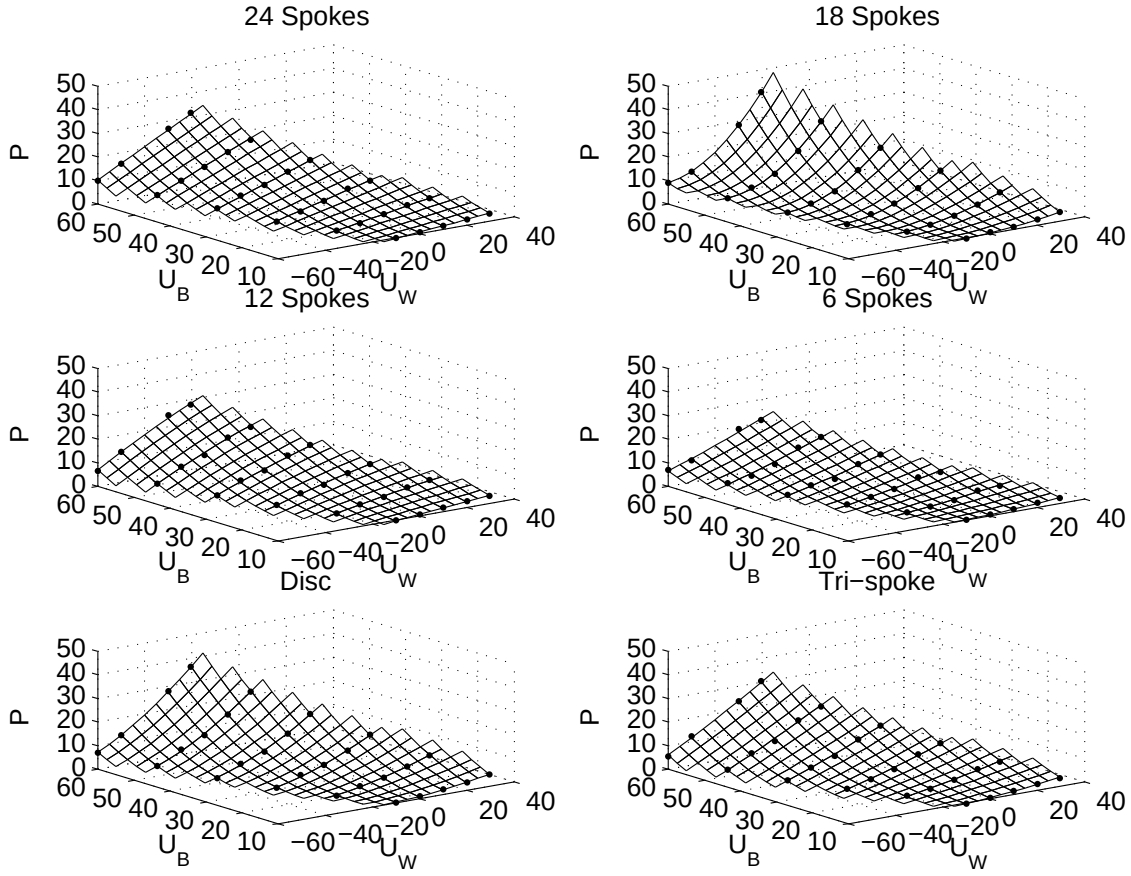

Figure 5: P for each configuration at varying U_B and U_W.

drag reduction is likely to be analogous to active flow control methods in aerodynamic design where the flow is modified by the introduction of jets, or by suction, to reduce drag due to turbulent flow. For the bicycle wheel, flow shed by the passing spokes is interacting with the axial flow over the wheel. At the critical spoke number it is likely that this interaction reduces the drag associated with the axial flow. While the rotational C_D maintains its generally linear increase with N_s (as seen in figure 7, the axial C_D displays a strong inflection at this point.

To put the results in this paper in context, we must compare them to the total power required to overcome the resistive force acting on the bicycle and rider. This can be

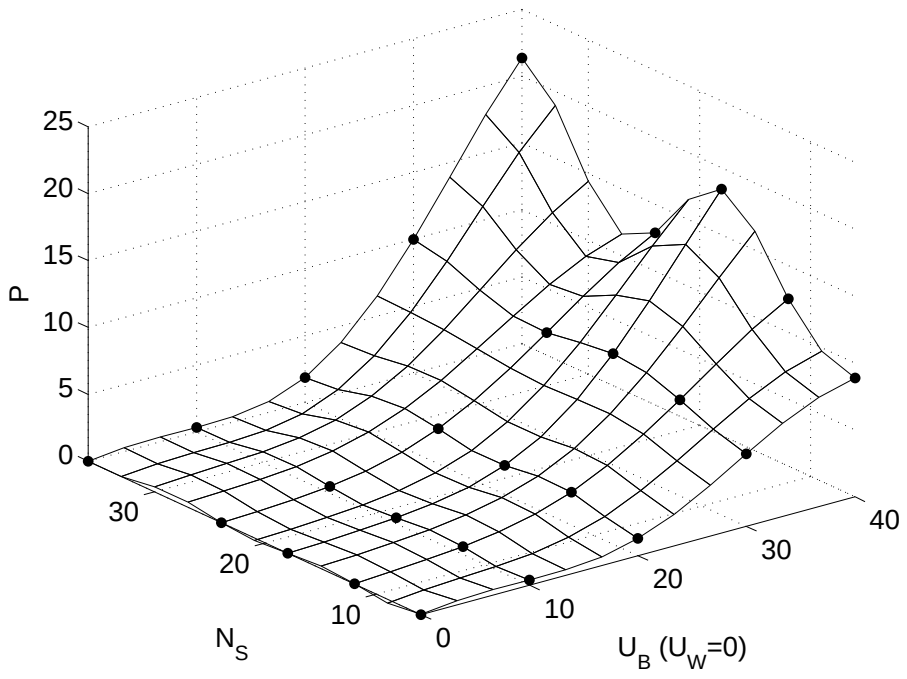

Figure 6: P for varying N_S and U_B.

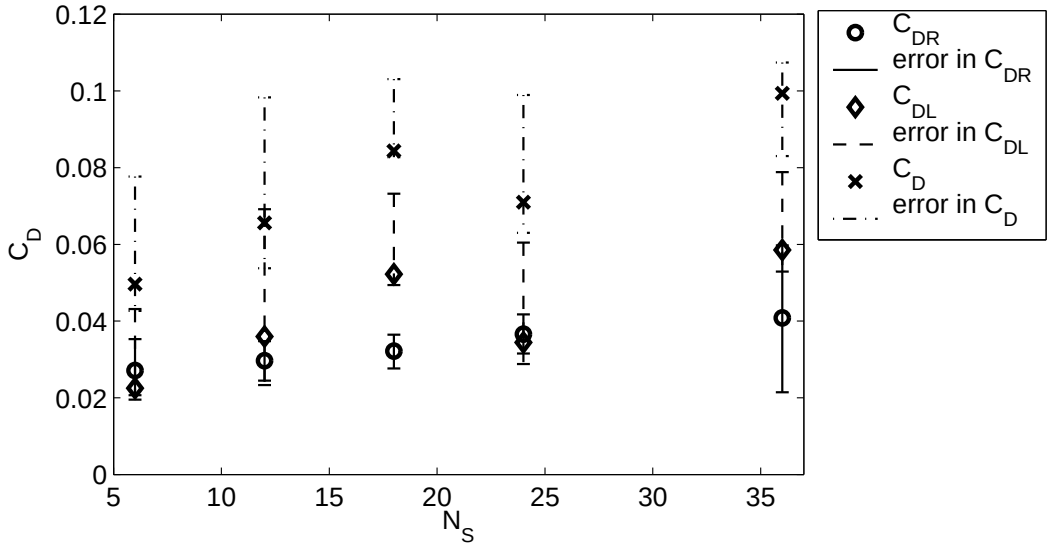

Figure 7: C_D variation with N_S. Error bars indicate errors in least squares and drag measurement.

expressed as

$$P = \frac{1}{2}\rho C_D A V^3 + C_R m g V, \tag{3}$$

where values for $C_D A$ are given by Grappe et al. (1997) for a cyclist riding a traditional frame with spoked wheels (spoke numbers are not given) in an upright position (hands on the top of the handlebars) with $C_D A = 0.299$, in a tucked position using conventional dropped handlebars $C_D A = 0.276$, and on triathlon style bars (the position used by Greg Lemond) $C_D A = 0.262$. They also tested Obree's first position (chest on hands with elbows tucked in and the trunk horizontal) and obtained $C_D A = 0.216$, although this is now banned in international races. The rolling resistance coefficient, C_R is given in the same reference as varying from 0.003 to 0.008 depending on the surface. We will use $C_R = 0.005$, $m = 70$ kg and $g = 9.81$. The total power required to ride in the four different positions is shown in figure 8. The power required to overcome the rolling resistance is also shown. The figure is truncated at 450W, which is the power sustainable by a world class cyclist for one hour (Chris Boardman averaged 442 W during his 1996 hour record of 56.375 km). It is clear how much effect a change in position can have on an event such as the hour record – particularly the use of the now banned Obree position. The power to overcome the drag of our worst wheel (36 spokes) and our best wheel (six spokes) indicates that a change in spoke configuration could have a similarly large effect. The powers are given for two wheels, although we cannot be sure that the drag reduction for the rear wheel will be as great as for the front. While a change from an upright position to triathlon style bars results in a drag reduction of 12%, a similar drag reduction might be achieved with a reduction from 36 to six spokes.

When selecting the number of spokes to be used, the results here must be coupled with the type of rider, terrain and speed of race and also the UCI regulations. For example, a strong heavy rider competing in a race over cobbles will be more concerned with durability than drag. A mountainous race with speeds below 20 $\mathrm{km \cdot hr^{-1}}$ when riding uphill will not be unduly affected by N_S (downhill speed is limited more by rider skill and nerve rather than aerodynamic drag). However, in an individual track race where durability is less important and there are no restrictions, the use of $N_S = 6$ may be advantageous. For the

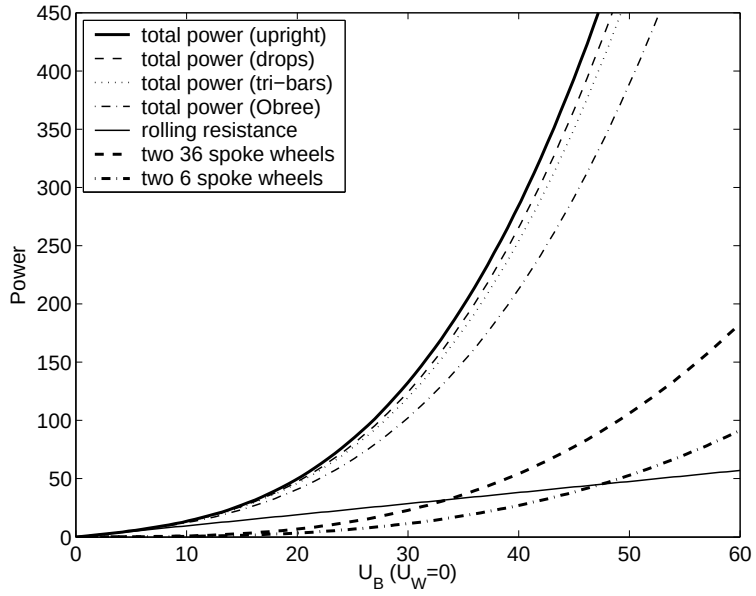

Figure 8: Power for various rider positions at varying U_B compared with power to overcome drag of wheels.

new hour record the rules allow as few as 16 spokes, but the results in this paper suggest $N_S \in \{24, 28\}$ would give better results.

4 Conclusion

In this short communication the importance of the choice of wheel configuration has been demonstrated along with the counter intuitive nature of the performance of different wheels. Although we cannot test every possible permutation, it has been shown that for the generic wheel tested here, there is a power minimum in the 24 to 36 spoke range. The results presented can help in the selection of wheel configuration for specific race conditions. The drag characteristics of bicycle wheels is undoubtedly an interesting area of research and further investigations in this area, either of an experimental or computational nature, would be welcome.

References

Freeman, B. C. (1980). Blockage corrections for bluff bodies in confined flows. Technical Report 80024, ESDU. Ammended 1998.

Grappe, F., Candau, R., Belli, A.,Rouillon, J. D. (1997). Aerodynamic drag in field cycling with special reference to the Obree's position. *Ergonomics*, **40**,1299–1311.

Greenwell, D. I., Wood, N. J., Bridge, E. K. L.,Addy, R. J. (1995). Aerodynamic characteristics of low drag bicycle wheels. *Aeronautical Journal*, **99**,109–120.

Jones, D. R. (2001). A taxonomy of global optimization methods based on response surfaces. *Journal of Global Optimization*, **21**,345–383.

Sayers, A. T.Stanley, P. (1994). Drag force on rotating cycle wheels. *J. Wind Eng. Ind. Aerodynamics*, **53**,431–440.

Tew, G. S.Sayers, A. T. (1999). Aerodynamics of yawed racing cycle wheels. *J. Wind Eng. Ind. Aerodynamics*, **82**,209–222.

UCI (2005). UCI cycling regulations. *Union Cycliste Internationale, www.uci.ch*.